

Supporting Information for

A Roadmap to Design Mechanically Robust Copolymer Hydrogels Naturally Cross-Linked by Hydrogen Bonds

Cagla ERKOC,¹ Erol YILDIRIM,² Mine YURTSEVER,¹ * and Oguz OKAY¹ *

¹Istanbul Technical University, Department of Chemistry, 34469 Maslak, Istanbul, Turkey.

²Middle East Technical University, Department of Chemistry, 06800 Ankara, Turkey

Table of Contents

Synthesis and Characterization of the Hydrogels	(S2)
Computational Methods	(S4)
Table S1. DFT optimized structures of monomer-water complexes and BSSE corrected H-bond energies in kcal/mol/H-bond.	(S5)
Table S2. log <i>P</i> per solvent accessible surface area (SA Å ²) for the MAAC, AAC, and NVI monomers and pentamers in neutral and ionized forms.	(S6)
Table S3. Monomer-monomer and water-monomer mixing energies, <i>E</i> _{mix} (in kcal/mol) and coordination numbers.	(S7)
Table S4. Total free energy of solvation (in kcal/mol) of the monomer.	(S7)
Table S5. The snapshot pictures of equilibrium structure of MAAC ₉ NVI ₁ , MAAC ₄ NVI ₁ , and AC ₄ NVI ₁ copolymers from the MD simulations.	(S8)
Table S6. <i>E</i> _{elec} and <i>E</i> _{vdW} (in kcal/mol) for the MAAC, AAC, and NVI monomers and pentamers in neutral and ionized forms.	(S9)
Table S7. Calculated monomer-monomer and water-monomer mixing energies <i>E</i> _{mix} at 298 K for the components of the copolymer hydrogels.	(S9)
Figure S1. The stress-strain curves, mechanical parameters, tensile cyclic tests, and hysteresis energies of homopolymer hydrogels.	(S10)
Figure S2. RDFs of polymer-water interactions of MAAC/DMAA and AAC/DMAA.	(S10)
Figure S3. Five successive loading-unloading cycles for AAC/NVI hydrogels at various NVI contents as indicated.	(S11)
Figure S4. Five successive loading-unloading cycles for MAAC/NVI hydrogels at various NVI contents as indicated.	(S11)
Figure S5. RDFs of polymer-water and polymer-polymer interactions in AAC/DMMA and AAC/NVI hydrogels by MD trajectory analysis.	(S12)
Figure S6. Five successive loading-unloading cycles for AAm/NVP (a), and MAAC/NVP hydrogels (b) at various NVP contents as indicated.	(S13)
Figure S7. Hysteresis energies and the fraction of dissipated energy per loading energy of AAm/NVP and MAAC/NVP hydrogels at various compositions plotted against the cycle number	(S14)
Figure S8. Shear rate dependence of the viscosities of solubilized hydrogels.	(S15)

Synthesis and Characterization of the Hydrogels

Materials. Methacrylic acid (MAAc, 99%, Merck), N,N-dimethylacrylamide (DMAA, 99%, Sigma-Aldrich), 1-vinylimidazole (NVI, 99%, Merck), N-vinyl pyrrolidone (NVP, 98%, Merck), acrylamide (AAm, 99%, Merck), 2-hydroxy-4'-(2-hydroxyethoxy)-2-methylpropiophenone (Irgacure 2959, 98%, Sigma-Aldrich), and poly(ethylene glycol) (PEG, 10,000 g·mol⁻¹, Sigma-Aldrich) were used as received. Acrylic acid (AAc, 99%, Merck) was freed from its inhibitor by passing through an inhibitor removal column (Sigma-Aldrich). The copolymer hydrogels were prepared by UV-initiated solution polymerization of the following comonomer pairs at various compositions: MAAc/DMAA, AAc/DMAA, AAc/NVI, MAAc/NVI, MAAc/NVP, and AAm/NVP. The reactions were carried out at 23±2 °C in the presence of 0.2 mol % Irgacure 2959 initiator (with respect to the monomers) under UV light at 360 nm for 24 h. The total monomer concentration was fixed at 40 wt %. Typically, to prepare MAAc/DMAA copolymer hydrogels with 20 mol % DMAA, MAAc (3.10 g) and DMAA (0.90 g) were dissolved in 6.0 g of water at room temperature. After dissolving Irgacure 2959 (20.3 mg), the solution was transferred into several 1 mL plastic syringes of 4.6 mm internal diameter, and the polymerization reactions were conducted in a UV reactor at 23±2 °C for 24 h under UV light at 360 nm.

Characterization. For the swelling tests in water, the as-prepared hydrogels were taken out of the syringes and cut into cylindrical specimens with a diameter of 4.6 mm and a length of around 3 mm. They were then immersed in excess distilled water for at least two weeks during which water was refreshed every second day. The swelling equilibrium of the samples was checked by weighing the specimens. The equilibrium swelling ratio m_{rel} was calculated as m/m_o where m and m_o are the masses of the specimen after equilibrium swelling and after preparation, respectively.

The solubilization of the hydrogels was carried out by immersing as-prepared hydrogel specimens in an excess of aqueous 7 M urea solution under stirring for 2 weeks at 23±2 °C. Except MAAc/NVI hydrogels, all copolymer hydrogels could be dissolved in this solution. The solubilization tests conducted in various aqueous solutions revealed that the MAAc/NVI gel specimens can easily be dissolved in alkaline solutions of pH > 11. A 0.1 M aqueous NaOH solution of pH = 12 was selected for the solubilization tests. The homogeneous polymer solutions thus obtained were then poured into dialysis tubes (10K MWCO, SnakeSkin, Pierce) and dialyzed for 3 days against water, an additional 1 day against 15 w/v % PEG-10000 to concentrate the solution. The concentrated solution was then freeze-dried on a Christ Alpha 2-4 LDplus freeze-dryer. For the viscosity measurements, 20 mg of the copolymers isolated from the hydrogels were dissolved in 2 mL of distilled water. The viscosities η of the copolymer solutions were measured at 25 °C on a Gemini 150 rheometer system, Bohlin Instruments, with a Peltier system for

temperature control. A cone-and-plate geometry with a cone angle of 4° and diameter of 40 mm over the range of shear rates 1×10^{-3} to $1 \times 10^2 \text{ s}^{-1}$.

The uniaxial tensile tests were conducted on hydrogel specimens of 4.6 mm in diameter and 60 mm in length. The tests were performed at $23 \pm 2 \text{ }^\circ\text{C}$ on a Zwick Roell Z0.5 TH test machine using a 500 N load cell. The initial sample length between the jaws was fixed at $10.0 \pm 0.1 \text{ mm}$. The tests were conducted at a constant crosshead speed of 10 and $50 \text{ mm} \cdot \text{min}^{-1}$ below and above 15% strain, respectively. From the load and displacement data, the nominal stress σ_{nom} , which is the force per cross-sectional area of the undeformed gel specimen, and the strain ε (deformed length / original length) were calculated. Young's modulus E was calculated from the slope of the stress-strain curves between 5 and 15% strain. The energy to break W (toughness) was calculated from the area under the stress-strain curves up to the fracture point. Cyclic tensile tests were conducted at a fixed crosshead speed of $50 \text{ mm} \cdot \text{min}^{-1}$ up to a maximum strain of 250%. All copolymer hydrogels were subjected to five successive tensile cycles with a waiting time of 1 min between cycles. Because of the rapid drying of MAAc/DMAA, AAc/NVI, and MAAc/NVI hydrogels, their cyclic mechanical tests were conducted after coating the specimens with silicon oil before the tests.

Computational Methods

The total energy of the copolymers is calculated by summing up all the bonded and non-bonded interactions in the copolymer systems. The major contributors of the non-bonded interactions are van der Waals (vdW) and electrostatic interactions which include H-bond interactions.

$$E_{\text{total}} = E_{\text{bonded}} + E_{\text{nonbonded}} \quad (\text{S1})$$

$$E_{\text{total}} = E_{\text{bonded}} + E_{\text{elec}} + E_{\text{vdW}} \quad (\text{S2})$$

Monomer-monomer, monomer-water mixing energies were calculated using the extended Flory-Huggins (FH) theory. The mixing of two units (denoted by i and j) is similar to a chemical reaction in which a bond between i and j is formed at the expense of i - i and j - j bonds. Let ω_{ij} , ω_{ii} , and ω_{jj} represent the energies associated with these respective bonds, the change in energy $\Delta\omega_{ij}$ for the formation of an i - j bond is given by

$$\Delta\omega_{ij} = \omega_{ij} - 0.5 (\omega_{ii} + \omega_{jj}) \quad (\text{S3})$$

The mixing energies E_{mix} can be calculated from $\Delta\omega_{ij}$ by

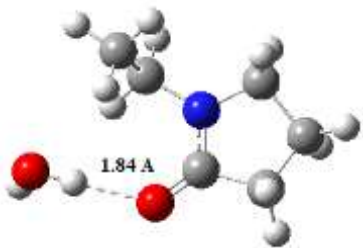
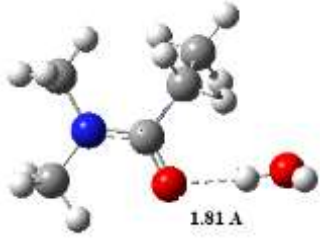
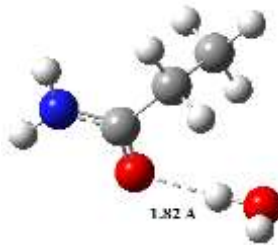
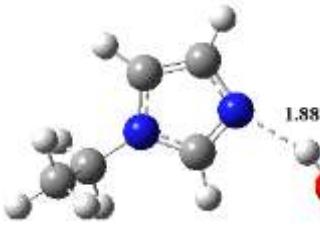
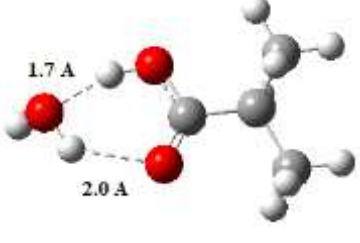
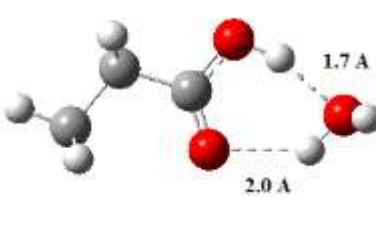
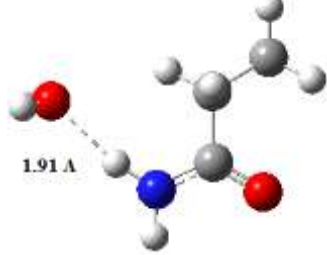
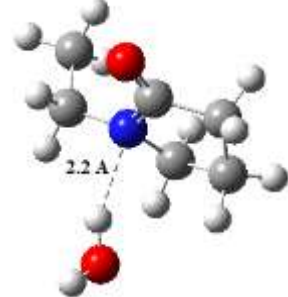
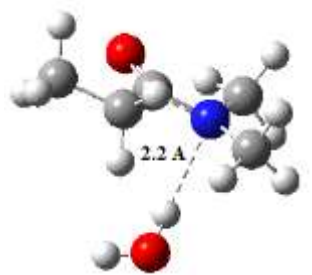
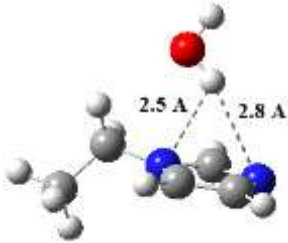
$$E_{\text{mix}} = \Delta\omega_{ij} Z_{ij} \quad (\text{S4})$$

where Z_{ij} is the coordination number. Monomer-monomer and water-monomer mixing energies, E_{mix} (in kcal/mol) and coordination numbers are given in Table S3.

Free energy of solvation was calculated for trimers of the six units in explicit water under periodic boundary condition based on the thermodynamic integration algorithm with coupling parameter method. The free energy of solvation was determined in three steps in this algorithm:^{S1} as a first step, the trimers were set as solute and discharged in the vacuum, and the free energy change associated with this discharge was determined, called ideal free energy of solvation. Then the neutral solute trimers were brought into contact with the water molecules. The free energy change for this discharged interaction was determined, known as vdW free energy of solvation. Next, the solvated and discharged solute molecule is charged again in solvent to determine the electrostatic free energy of solvation. All cells have been constructed at water density and simulated by COMPASS force field. Total free energy of solvation was calculated as the sum of the free energy contributions from ideal, vdW and electrostatic free energies of solvation. The results of calculations (in kcal/mol) are given in Table S4.

(S1) Steinbrecher T.; Joung, I. S.; Case, D. A. Soft-Core Potentials in Thermodynamic Integration. Comparing One- and Two-Step Transformations., J. Comp. Chem., 2011, 32, 3253-3263.

Table S1. DFT optimized structures of monomer-water complexes and BSSE corrected H-bond energies in kcal/mol/H-bond. The H-bond distances (in Å) are shown on the H-bonds (dotted lines).^a

Monomer-Water Complexes	E_{Hbond}	Monomer-Water Complex	E_{Hbond}
 <p>NVP</p>	-7.88	 <p>DMAA</p>	-7.86
 <p>AAM</p>	-7.32	 <p>NVI</p>	-7.27
 <p>MAAc</p>	-6.38	 <p>AAc</p>	-6.34
 <p>AAm</p>	-5.91	 <p>NVP</p>	-5.35
 <p>DMAA</p>	-4.89	 <p>NVI</p>	-2.92

^a The complexes were modeled by placing water molecule nearby possible H-bond donor and acceptor atoms of the monomers. Then, the geometries of the H-bonded complexes were optimized at M06-2X/6-31g(d,p) level of the theory. The Counterpoise method has been employed to calculate the basis set

superposition error (BSSE)-corrected complexation energies, which then tabulated as H-bond energies. Sterically unhindered carbonyl oxygens and pyridinic nitrogen atoms form the most strong H-bonds with water through their hydrogen atoms. The strong H-bond energies ranges between 7-8 kcal/mol per H-bond. The pyrrolic nitrogen atom of NVI and methyl substituted nitrogen atoms form weaker H-bonds at larger H-bond distances than 2.0 Å due to the steric hinderence of the methyl groups.

Table S2. $\log P$ per solvent accessible surface area (SA, Å²) for the monomers and pentamers in neutral and ionized forms, and water.

	10 ³ log P /SA (monomer)	10 ³ log P /SA (pentamer)
MAAc	3.52	4.82
AAc	1.98	1.42
NVI	0.968	-0.508
DMAA	0.843	-0.29
NVP	0.602	-0.940
AAm	-0.690	-3.70
AAc ⁻	-4.49	-10.8
MAAc ⁻	-2.15	-6.98
NVI ⁺	0.325	-1.53
water	-2.97	-2.97

Table S3. Monomer-monomer and water-monomer mixing energies, E_{mix} (in kcal/mol) and coordination numbers.

Monomer _i	Monomer _j	E_{mix}	E_{ii}	E_{ij}	E_{jj}	Z_{ii}	Z_{ij}	Z_{ji}	Z_{jj}
NVP	AAM	-2.75	-2.46	-3.91	-4.41	5.13	5.62	4.32	4.71
NVP	MAAc	-2.15	-2.46	-3.28	-3.29	5.13	5.51	4.6	4.93
DMAA	AAc	-0.49	-2.23	-2.86	-3.36	4.92	5.29	4.34	4.65
NVI	AAc	-0.46	-2.79	-3.16	-3.38	4.99	5.3	4.39	4.66
DMAA	MAAc	-0.36	-2.23	-2.82	-3.27	4.92	5.17	4.7	4.92
NVI	MAAc	-0.31	-2.79	-3.09	-3.27	4.99	5.17	4.75	4.93
water	MAAc	1.61	-2.31	-2.34	-3.31	5.51	3.73	7.29	4.93
water	AAc	1.56	-2.31	-2.41	-3.38	5.51	3.83	6.69	4.66
water	AAM	-0.28	-2.31	-3.2	-4.41	5.51	3.82	6.8	4.71
water	DMAA	-2.09	-2.31	-2.48	-2.23	5.51	3.54	7.68	4.92
water	NVP	-6.04	-2.31	-3.2	-2.46	5.51	3.45	8.26	5.13
water	NVI	-3.25	-2.31	-2.93	-2.78	5.51	3.57	7.71	4.99

Table S4. Total free energy of solvation (in kcal/mol) of the monomer.

Monomer	Total solvation free energy <i>Force field charges</i>	Total solvation free energy <i>With DFT charges</i>
MAAc	-10.818	-14.037
AAc	-12.159	-14.879
AAM	-14.083	-17.624
DMAA	-4.447	-9.859
NVP	-5.654	-15.247
NVI	-10.272	-18.100

Table S5. The snapshot pictures of equilibrium structure of MAAc₉NVI₁, MAAc₄NVI₁, and AAc₄NVI₁ copolymers from the MD simulations.

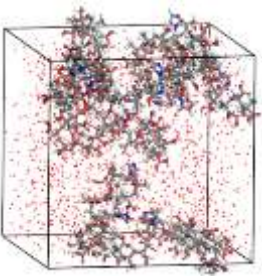
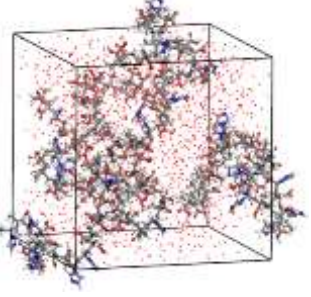
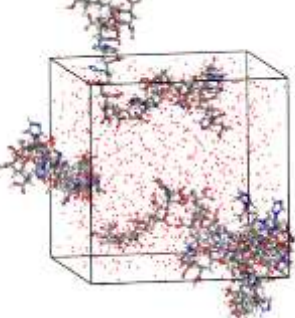
Copolymer	logP	E _{elec} /atom (kcal/mol)
MAAc ₉ NVI ₁		-2.96
MAAc ₄ NVI ₁		-2.93
AAc ₄ NVI ₁		-3.34

Table S6. E_{elec} and E_{vdW} (in kcal/mol) for the MAAc, AAc, and NVI monomers and pentamers in neutral and ionized forms.

Copolymer	E_{elec}	E_{vdW}	$E_{\text{vdW}}/E_{\text{total}}$	$E_{\text{elec}}/E_{\text{total}}$	$E_{\text{elec}}/E_{\text{nonb}}$
AAc/NVI (4/1)	-3.34	0.49	-0.22	1.52	1.17
AAc ⁻ /NVI ⁺ (4/1)	-3.81	0.54	-0.21	1.50	1.16
AAc/NVI (9/1)	-3.45	0.51	-0.22	1.51	1.11
AAc ⁻ /NVI ⁺ (9/1)	-3.68	0.52	-0.21	1.50	1.17
MAAc/NVI (9/1)	-2.96	0.56	-0.35	1.86	1.23
MAAc ⁻ /NVI ⁺ (9/1)	-3.14	0.58	-0.34	1.83	1.23
MAAc/NVI (4/1)	-2.93	0.54	-0.33	1.82	1.22
MAAc ⁻ /NVI ⁺ (4/1)	-3.30	0.58	-0.31	1.78	1.21

Table S7. Calculated monomer-monomer and water-monomer mixing energies E_{mix} (in kcal/mol) at 298 K for the components of the copolymer hydrogels.

i	j	E_{mix}^{ij}
NVI	AAc	-0.46
NVI ⁺	AAc ⁻	-534.96
NVI	MAAc	-0.31
NVI ⁺	MAAc ⁻	-546.42

water	MAAc	1.61
water	MAAc ⁻	-134.89
water	AAc	1.56
water	AAc ⁻	-126.92
water	NVI	-3.25
water	NVI ⁺	-122.79

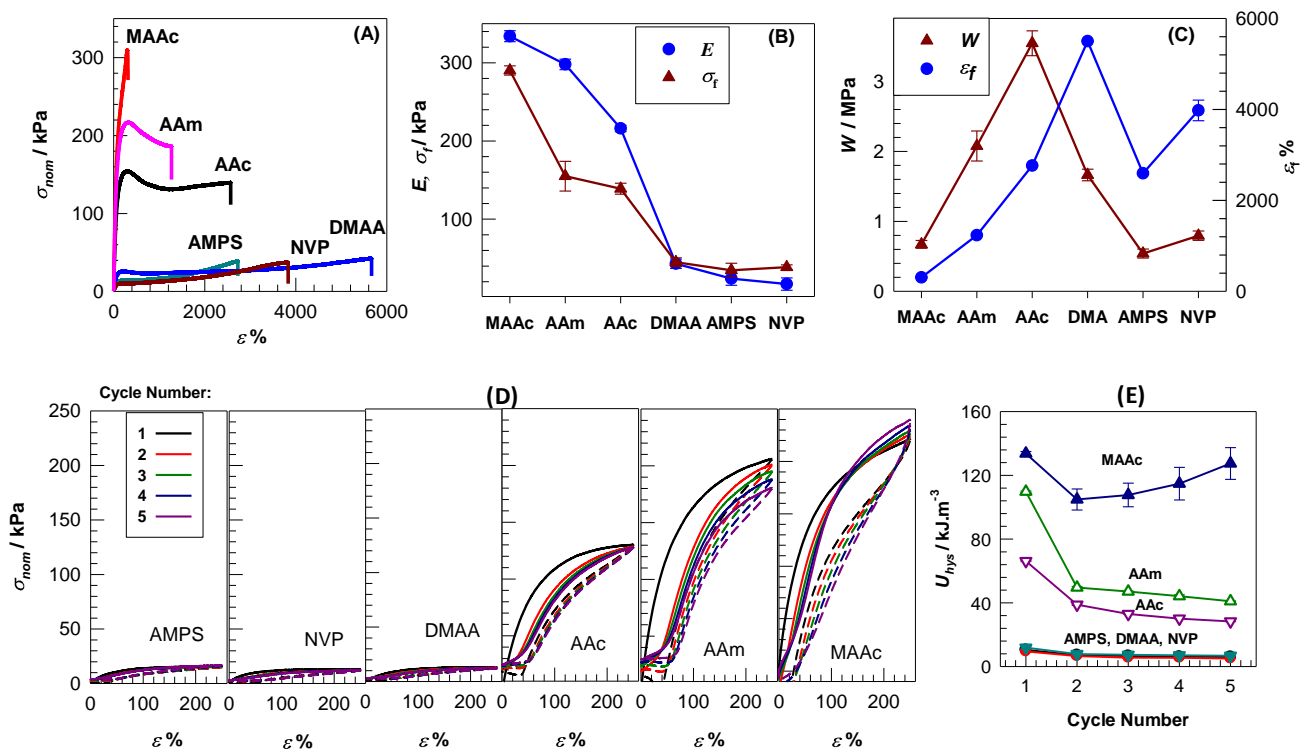


Figure S1. The stress-strain curves (A), mechanical parameters (B, C), tensile cyclic tests (D), and hysteresis energies U_{hys} of homopolymer hydrogels. The starting monomers are indicated. The test conditions are the same as the comonomer hydrogels given in the text.

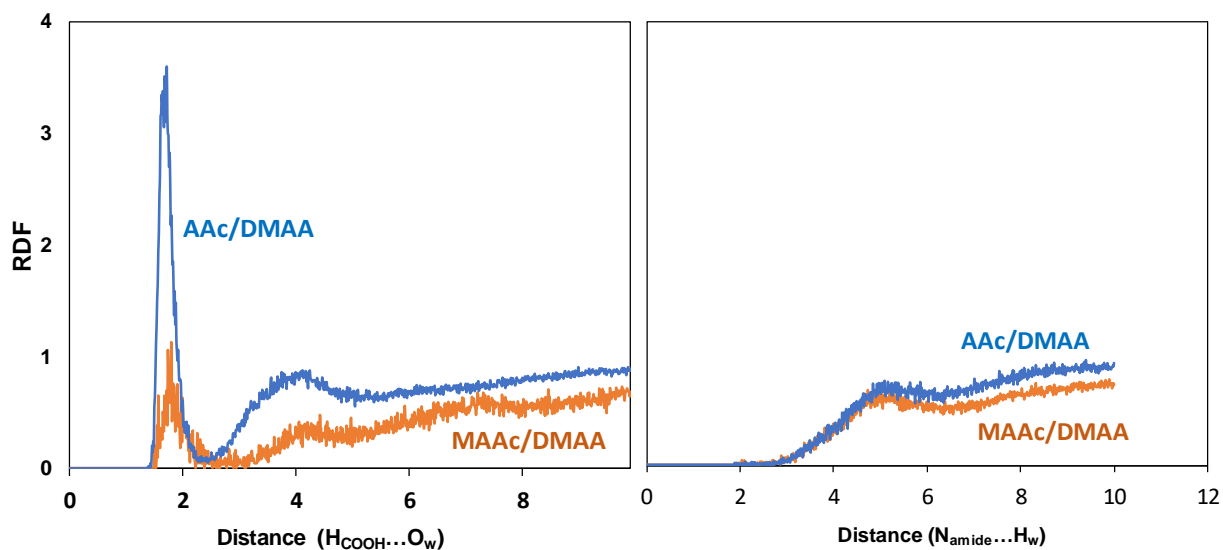


Figure S2. RDFs of polymer-water interactions of MAAc/DMAA and AAc/DMAA hydrogels.

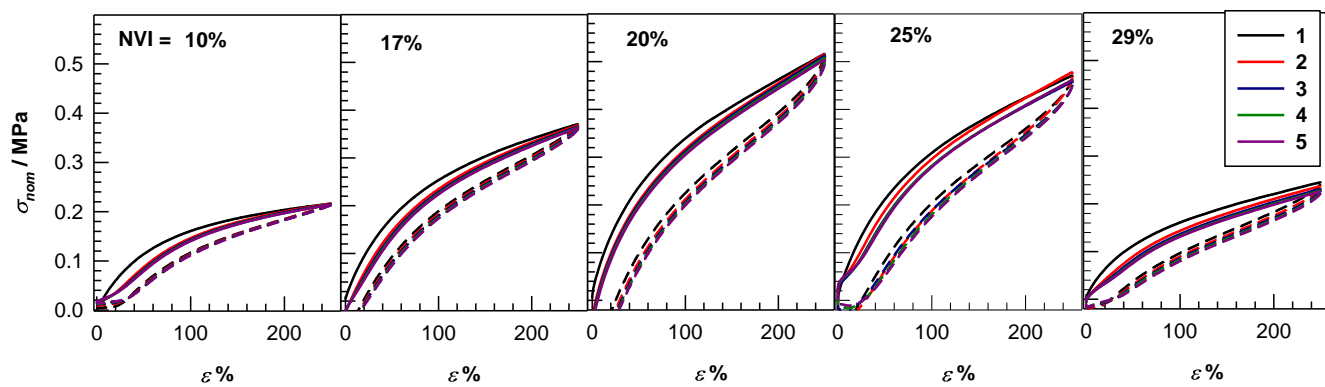


Figure S3. Five successive loading-unloading cycles for AAc/NVI hydrogels at various NVI contents as indicated. Loading and unloading curves are shown by the solid and dashed lines, respectively.

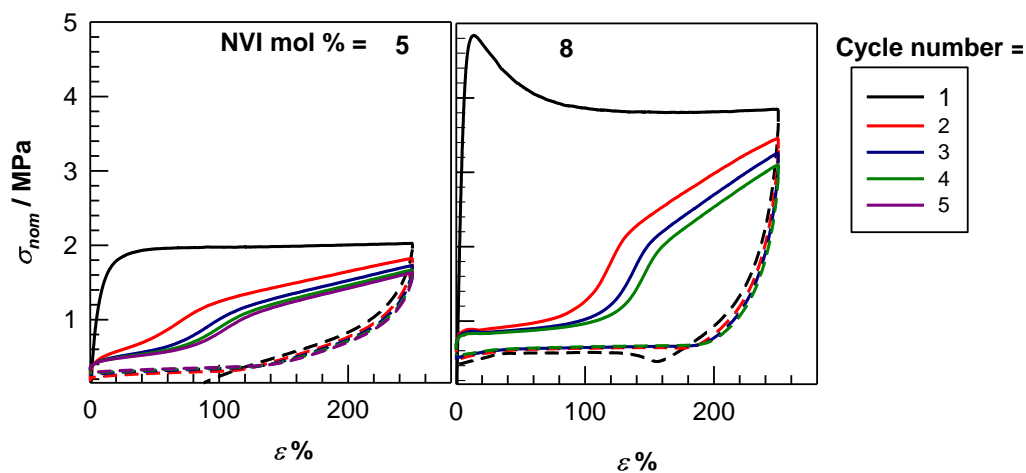


Figure S4. Five successive loading-unloading cycles for MAc/NVI hydrogels at various NVI contents as indicated. Loading and unloading curves are shown by the solid and dashed lines, respectively.

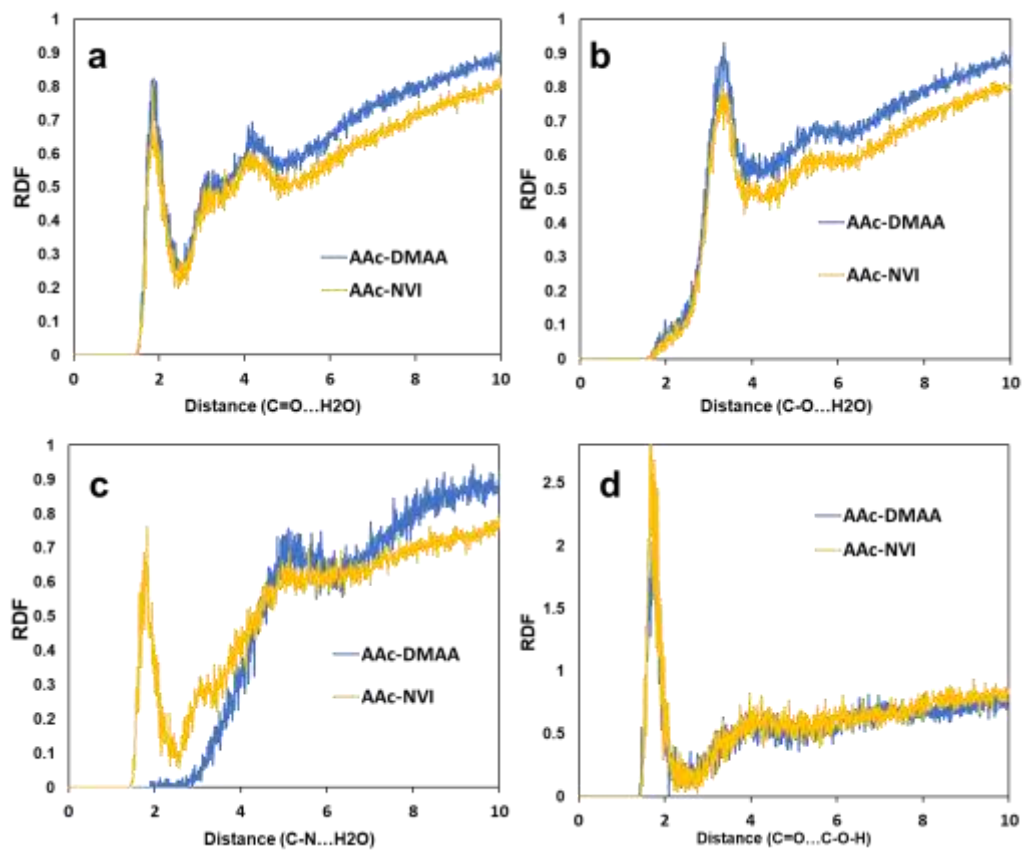


Figure S5. RDFs of polymer-water and polymer-polymer interactions in AAc/DMAA and AAc/NVI hydrogels at 4/1 molar ratio by MD trajectory analysis.

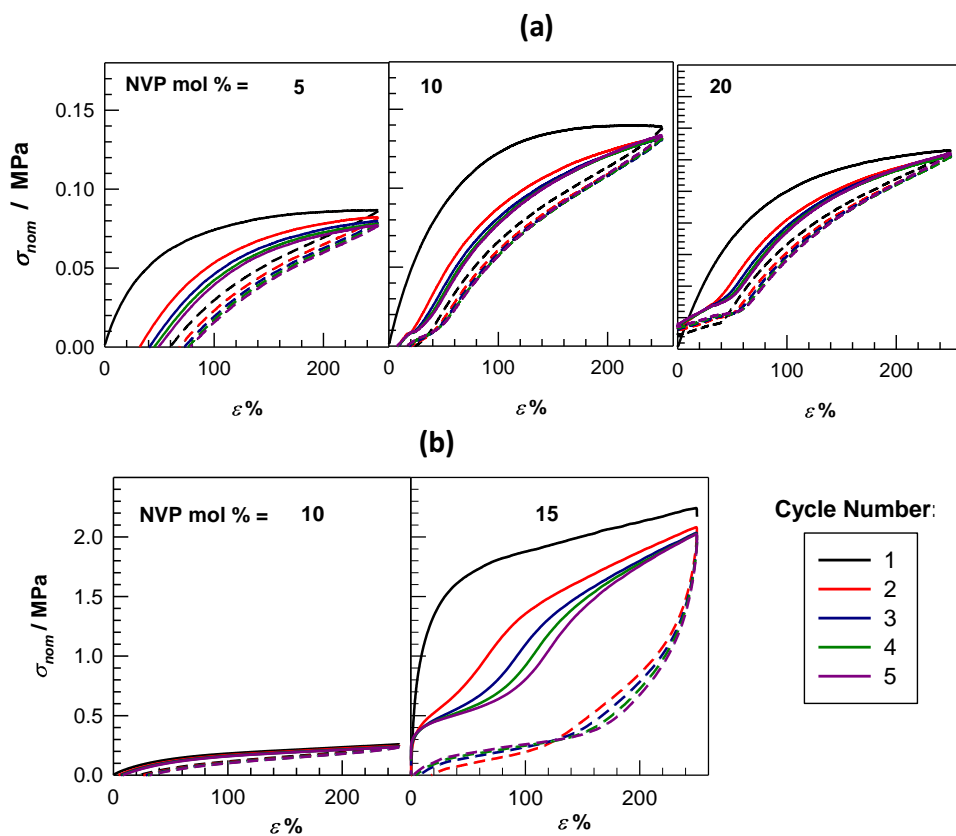


Figure S6. Five successive loading-unloading cycles for AAm/NVP (a), and MAAC/NVP hydrogels (b) at various NVP contents as indicated. Loading and unloading curves are shown by the solid and dashed lines, respectively.

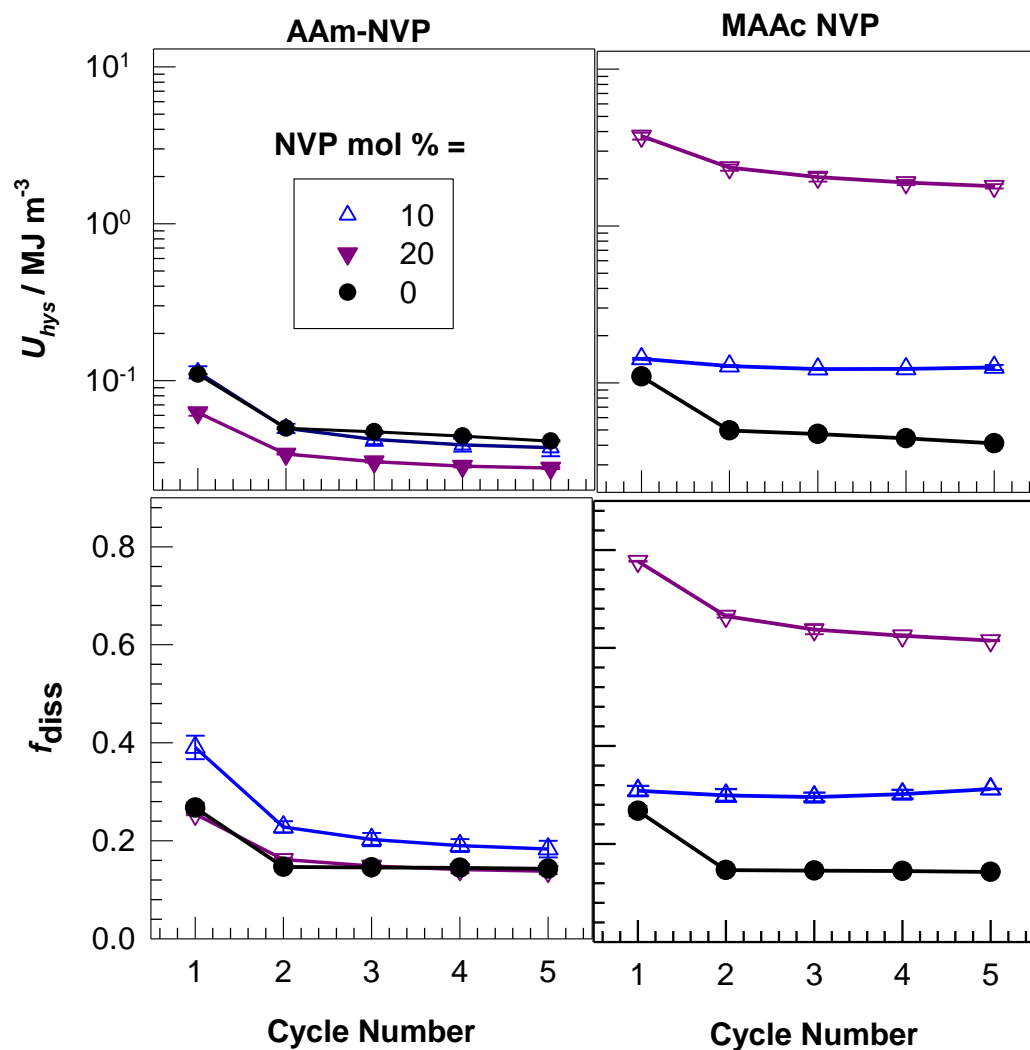


Figure S7. Hysteresis energies U_{hys} , and the fraction of dissipated energy per loading energy f_{diss} of AAm/NVP (left) and MAAC/NVP hydrogels (right) at various compositions plotted against the cycle number.

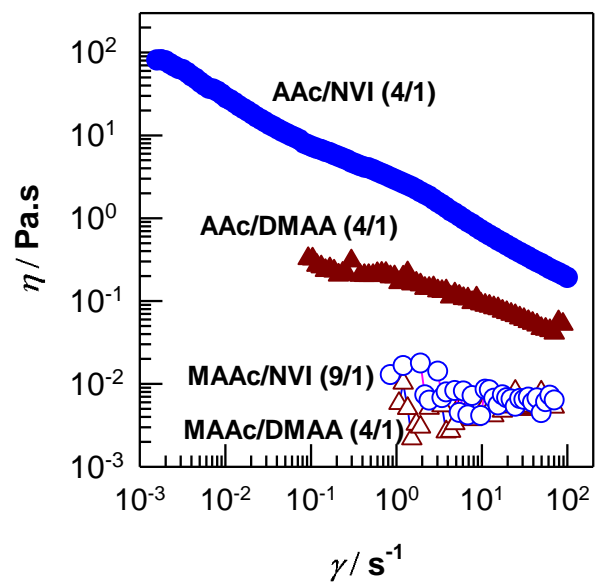


Figure S8. Shear rate dependence of the viscosities of solubilized copolymer hydrogels in water at 1 w/v% concentration. The type of the copolymers is indicated.